

# Effects of near-fault loading and lateral bracing on the behavior of RBS moment connections

Qi-Song “Kent” Yu†

*Degenkolb Engineers, San Francisco, CA 94104, U.S.A.*

Chia-Ming Uang‡

*Department of Structural Engineering, University of California, San Diego, La Jolla, CA 92093-0085, U.S.A.*

**Abstract.** An experimental study was conducted to evaluate the effects of loading sequence and lateral bracing on the behavior of reduced beam section (RBS) steel moment frame connections. Four full-scale moment connections were cyclically tested—two with a standard loading history and the other two with a near-fault loading history. All specimens reached at least 0.03 radian of plastic rotation without brittle fracture of the beam flange groove welds. Two specimens tested with the near-fault loading protocol reached at least 0.05 radian of plastic rotation, and both experienced smaller buckling amplitudes at comparable drift levels. Energy dissipation capacities were insensitive to the types of loading protocol used. Adding a lateral bracing near the RBS region produced a higher plastic rotation; the strength degradation and buckling amplitude were reduced. A non-linear finite element analysis of a one-and-a-half-bay beam-column subassembly was also conducted to study the system restraint effect. The study showed that the axial restraint of the beam could significantly reduce the strength degradation and buckling amplitude at higher deformation levels.

**Key words:** Northridge earthquake; reduced beam section (RBS) moment connection; steel moment connection; near-fault ground motion; loading protocol; lateral bracing, system restraint.

---

## 1. Introduction

Damage that was observed in a significant number of welded moment connections in steel moment frame structures after the 1994 Northridge, California earthquake led the engineers and researchers in the United States to develop alternative connection types. One such design—the reduced beam section (RBS) scheme which introduces a structural fuse in the steel beams by trimming some portion of the beam flanges near the column, can significantly enhance the seismic behavior of steel moment frame connections (Plumier 1997). Stable yielding of the beam and column panel zone can be developed by moving the beam plastic hinge region a short distance from the column face, thereby protecting the beam flange groove welds from brittle fracture. The effectiveness of the RBS moment connections has been demonstrated through numerous large-scale

---

†Ph.D.

‡Professor

testing (Chen *et al.* 1996, Engelhardt *et al.* 1998, Gilton *et al.* 2000). All of this testing, however, were conducted using "standard" loading protocols with a symmetric loading pattern of increasing amplitudes. Nevertheless, questions were raised after the Northridge earthquake regarding the effect of an earthquake occurring in the immediate vicinity of a building. One or two short-duration, high-amplitude pulses characterize this type of "near-fault" ground motion. Near-fault ground motions were shown to impose large deformation demand to the structure (Anderson and Bertero 1987, Hall 1998, Krawinkler and Gupta 1998). The effect of this type of ground motion on the behavior of RBS moment connections was not clear.

Questions were also raised concerning the need for extra lateral bracing for RBS beams. Some design engineers believed that lateral bracing should be provided near the RBS region because both the AISC seismic (1997) and plastic (1993) design provisions require lateral bracing at the plastic hinge location, and the weak-axis radius of gyration of the RBS is significantly reduced. Since adding lateral bracing near the RBS region increases the construction cost, some argued against it because available test results showed acceptable performance even though such lateral bracing was not provided near the RBS location, and the lateral bracing requirement in the AISC Seismic Provisions (1997) may be too conservative. It was also speculated that the floor slab might be beneficial in controlling lateral-torsional buckling, and the axial restraint in a building frame would limit the amount of beam buckling.

## 2. Objectives

The main objectives of this research were to evaluate experimentally both the effects of near-fault loading and extra lateral bracing on the cyclic response of steel RBS moment connections. A total of four nominally identical, full-scale steel beam-column subassemblies with the RBS moment connection design were constructed and tested quasi-statically (Yu *et al.* 1999). In addition, an analytical study of a beam-column subassembly representing a portion of a multistory moment frame was conducted to investigate the system axial restraining effects on the behavior of RBS moment connections.

## 3. Experimental program

### 3.1. Specimen design and fabrication

Four specimens, designated as LS-1 through LS-4, were tested with the setup shown in Fig. 1. Each specimen was consisted of a W14×176 column and a W30×99 beam. The design of the RBS moment connection was based on a procedure recommended by Engelhardt (1999) and the AISC Seismic Provisions (AISC 1997). The RBS moment connection details are illustrated in Fig. 2. Both the beam flanges and web were connected to the column with a full penetration groove weld. Continuity plates were provided, but no doubler plate was required in the column panel zone. Both LS-1 and LS-4 were tested with a standard loading protocol, while LS-2 and LS-3 were tested with a near-fault loading protocol. The beam of each specimen was braced laterally by a pair of guide columns, but an extra lateral brace was provided near the RBS region for LS-4 (see Fig. 3).

A572 Grade 50 steel with special requirements (now called A992 steel) per AISC Technical Bulletin No. 3 (AISC 1997) was specified for the beams and columns. The beams were from the

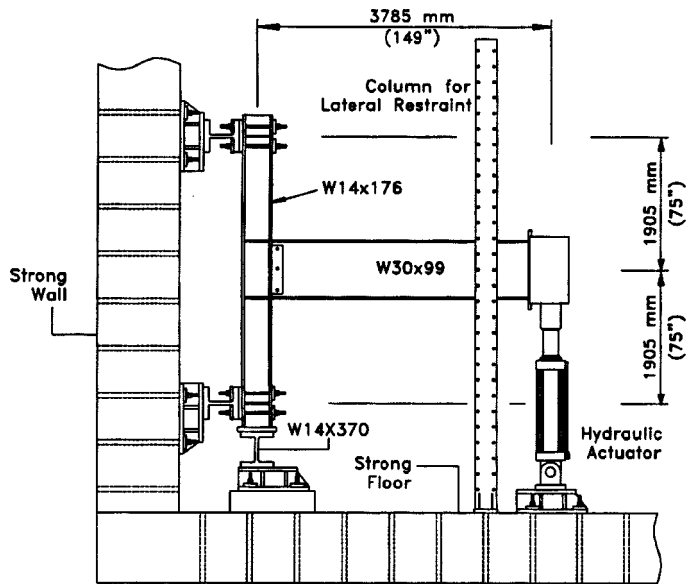


Fig. 1 Test setup

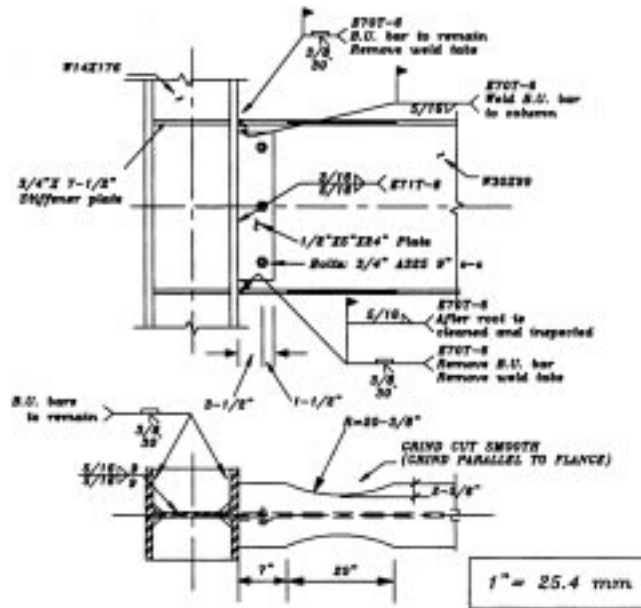


Fig. 2 RBS moment connection details

same heat of steel. The columns of Specimens LS-1 through LS-3 were from the same heat of steel. But the column of LS-4 was from a different heat of steel. Tensile coupons were cut from the members and tested according to the ASTM standard procedures, with the results shown in Table 1. The values from the certified mill test reports are also included in Table 1.

A commercial fabricator constructed the specimens. To simulate the field condition, the beam was

Table 1 Mechanical properties

Specimen	Member	Coupon	$F_y$ (MPa)	$F_u$ (MPa)	Elong.*
All	Beam W30×99	Flange	379	496	28%
		Web	400	517	26%
		Mill Cert.	386	510	26%
LS-1 to LS-3	Column W14×176	Flange	386	510	31%
		Web	372	503	28%
		Mill Cert.	400	524	21%
LS-4	Column W14×176	Mill Cert.	441	579	26%

\*Based on 203 mm (8 in.) gage length.

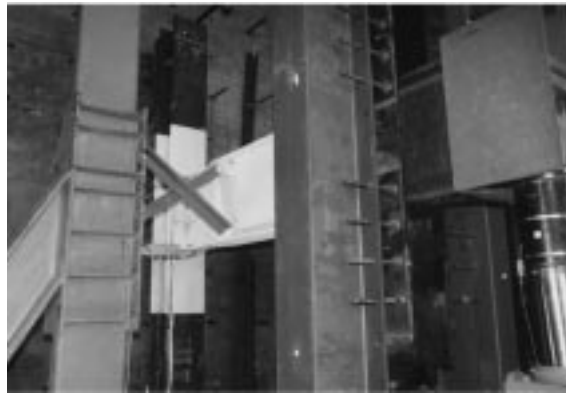


Fig. 3 Extra bracing for specimen LS-4

installed with three erection bolts and the moment connection was welded with the column in an upright position. All welding was performed with the self-shielded flux-cored arc welding process, using electrodes that have a specified minimum Charpy V-Notch impact value of 27.1 Joule (20 ft-lbs) at  $-28.8^{\circ}\text{C}$  ( $-20^{\circ}\text{F}$ ) (AISC 1997). A 1.8 mm (0.072 in) diameter E71T-8 (Lincoln NR-232) electrode was used for the complete joint penetration groove weld between the beam web and the column flange, and a 2.4 mm (3/32 in) diameter E70T-6 (Lincoln NR-305) electrode was used for the welds between the beam flanges and the column. The steel backing was removed from the beam bottom flange and the root pass back-gouged, refilled, and covered with a fillet weld from below. The steel backing was left on the beam top flange, but a fillet weld was applied between it and the column flange. Additional lateral bracing was provided to LS-4 at a location 152 mm (6 in) outside the RBS region. Lateral bracing was designed for 6% of the strength of the compression flange of the RBS section (Zekioglu *et al.* 1997). The bracing system was also designed to provide an equivalent axial stiffness of about 122.6 kN/mm (700 kips/in) at both top and bottom flange levels. Lateral bracing was designed such that it could move up and down with the beam.

### 3.2. Loading histories

Specimens LS-1 and LS-4 were tested with the standard SAC loading protocol (see Fig. 4)

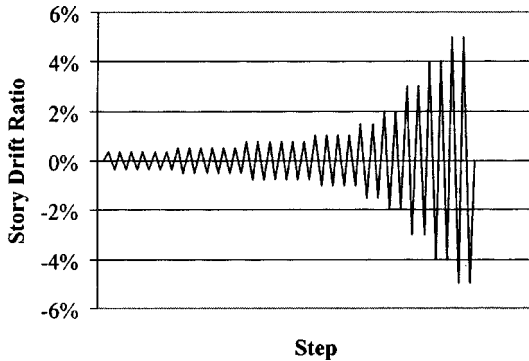


Fig. 4 SAC standard loading history

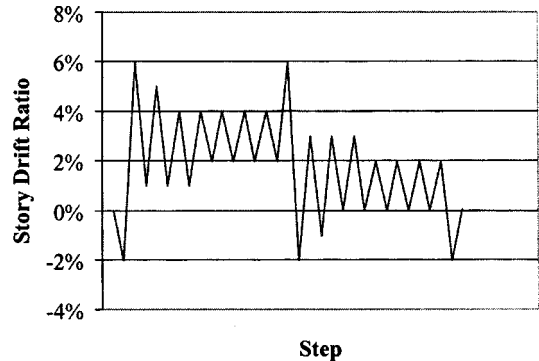


Fig. 5 SAC near-fault loading history

developed by Krawinkler (Clark *et al.* 1997). The loading sequence was controlled by the inter-story drift ratio, beginning with six cycles each of 0.375%, 0.5%, and 0.75% drift ratio. The next four cycles were at 1% drift, followed by two cycles of 1.5% drift. The sequence then completed two cycles each of successively increasing drift percentages (i.e., 2%, 3%, 4%, ...) until failure. The near-fault loading sequence for Specimen LS-3, also developed by Krawinkler, is shown in Fig. 5. The sequence begins with a pull in one direction to  $-2\%$  drift, followed by a large push to  $+6\%$  drift in the opposite direction. Then there is a single cycle between  $+1\%$  and  $+5\%$  and several cycles between  $+1\%$  and  $+4\%$ . (The load history up to this point approximately represents a complete structural response produced by a near-fault ground motion.) Following is a cycle from  $+6\%$  drift to  $-2\%$  drift. Next the load is pushed up to  $+3\%$  drift and cycled between  $+3\%$  and  $0\%$  drift for several cycles before the entire loading history is repeated if the strength does not degrade significantly. The same near-fault loading history was used for LS-2, but with the sign reversed.

## 4. Test results

### 4.1. Specimens LS-1 and LS-4: Standard loading protocol

Specimen LS-1 remained elastic through the cycles of 0.75% drift. Panel zone yielding began at about 1% drift, and minor web local buckling (WLB) was observed at 1.5% drift. Significant buckling occurred at 3% drift, with the amplitudes of lateral-torsional buckling (LTB) and WLB measured at 86 mm (3-1/4 in) and 30 mm (1-3/16 in), respectively. By the second cycle at 4% drift the LTB amplitude had increased to 114 mm (4-1/2 in), the WLB amplitude to 71 mm (2-13/16 in), and the beam flexural strength at the column face degraded just below 80% of the nominal plastic moment capacity of the unreduced beam section. The test was halted upon the completion of the third cycle of 5% drift due to significant strength degradation. Fig. 6(a) is a plot of the load versus beam tip displacement relationship. At the end of the test, the beam shortened by 38 mm (1-1/2 in) and 76 mm (3 in) at the beam top and bottom flange levels, respectively, due to buckling.

The behavior of Specimen LS-4 was similar to LS-1 up to 3% drift. After the second cycle of 3% drift, LTB and WLB amplitudes were measured at 78 mm (3-1/16 in) and 29 mm (1-1/8 in),

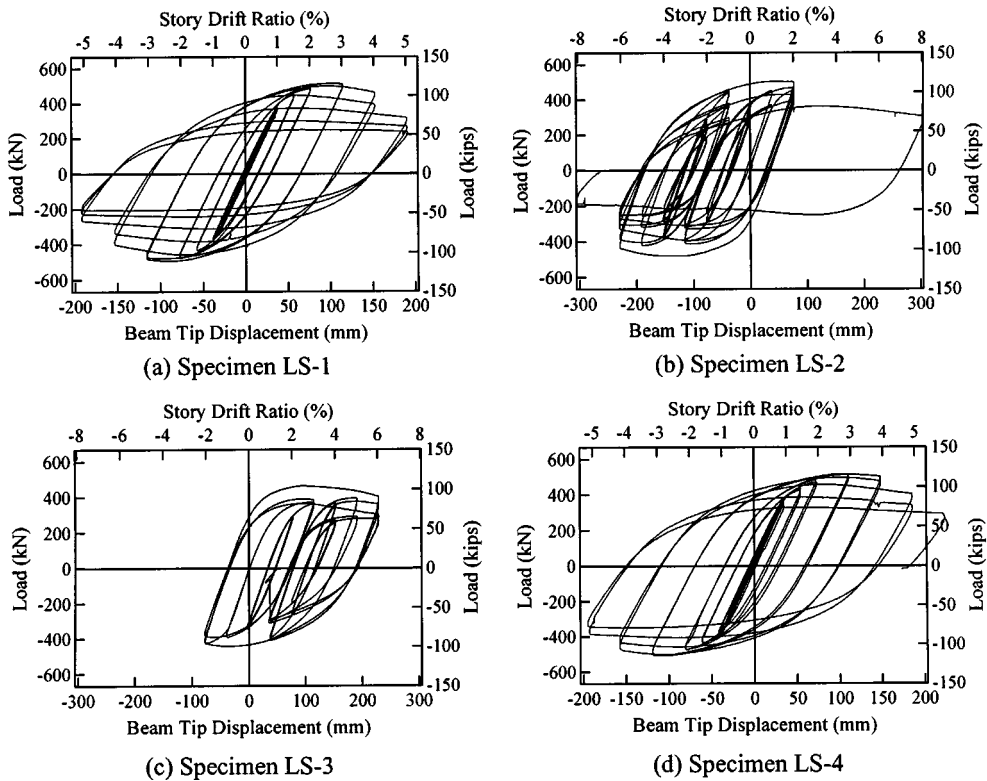


Fig. 6 Load versus beam tip displacement relationships

respectively. Beyond 3% drift, the connection strength began to degrade. Extra lateral bracing reduced the buckling amplitudes. At the end of the 4% drift cycles, LTB and WLB amplitudes had increased to only 89 mm (3-1/2 in) and 60 mm (2-3/8 in), respectively, and the strength had not significantly degraded. The testing continued through the 5% drift cycles, but was stopped during the first cycle of 6% drift due to the connection failure in the bracing system. Fig. 6(d) shows a plot of the load versus beam tip displacement relationship.

#### 4.2. Specimens LS-2 and LS-3: Near-fault loading protocol

Specimen LS-2 exhibited excellent performance under the near-fault loading history. Panel zone yielding was noticed during the first excursion to +2% drift. Significant buckling of the beam bottom flange was observed during the following excursion to -6% drift, with LTB reaching 89 mm (3-1/2 in), WLB reaching 52 mm (2-1/16 in), and flange local buckling (FLB) reaching 37 mm (1-7/16 in). The buckling amplitudes decreased during the following cycles to smaller drifts. When the -6% drift was imposed for the second time, the LTB, WLB, and FLB amplitudes further increased to 98 mm (3-7/8 in), 60 mm (2-3/8 in), and 49 mm (1-15/16 in), respectively. The following peak at +2% drift saw a decrease in the buckling of the bottom flange and significant yielding of the top flange. The buckling amplitudes stayed within a range just below the values of the initial buckling during the following cycles. The entire loading history was repeated for the second

time. Fissure-like cracks due to low-cycle fatigue were observed in the beam bottom flange at the RBS region. The entire loading history was applied for the third time. Soon after the first 6% drift peak (the fifth time) was applied the crack had propagated through half of the bottom flange, and the test was stopped. See Fig. 6(b) for a plot of the load versus beam tip displacement relationship.

The performance of LS-3 was very similar to that of LS-2. Panel zone yielding and significant buckling of the beam top flange near the RBS region occurred in the first two peaks. The amplitude of LTB was 114 mm (4-1/2 in), WLB was 60 mm (2-3/8 in), and FLB was 60 mm (2-3/8 in) after the second +6% drift. Fissure-like cracks were noticed at the third +6% peak, and the top flange of the beam fractured due to low-cycle fatigue after the +6% peak was imposed to the specimen for the fourth time. See Fig. 6(c) for a plot of the load versus displacement relationship. Both LS-2 and LS-3 experienced the near-fault loading history at least twice (i.e., at least four consecutive near-fault events) before low-cycle fatigue fracture occurred. In reality, this type of fracture is unlikely because of the low possibility of four large near-fault events in a row.

## 5. Implications of near-fault loading effects

### 5.1. Total plastic rotation and energy dissipation

The Acceptance Criteria in FEMA 267A (SAC 1996) was used to determine the plastic rotation capacity. The criteria require that the beam strength at the column face should not degrade below 80% of the nominal plastic moment of the unreduced beam section for one complete cycle. A summary of the total plastic rotation achieved in each specimen is included in Fig. 7. Both LS-1 and LS-4 reached a total plastic rotation 0.03 radian before significant strength degradation occurred. Specimens LS-2 and LS-3 reached a total plastic rotation of 0.05 radian in the direction of large excursion without significant strength degradation. The plastic rotation of these two specimens was limited by the amount of displacement imposed. A higher plastic rotation might have been achieved had a larger displacement applied to the specimens. Therefore, the RBS moment connections can easily accommodate the high deformation demand imposed by the near-

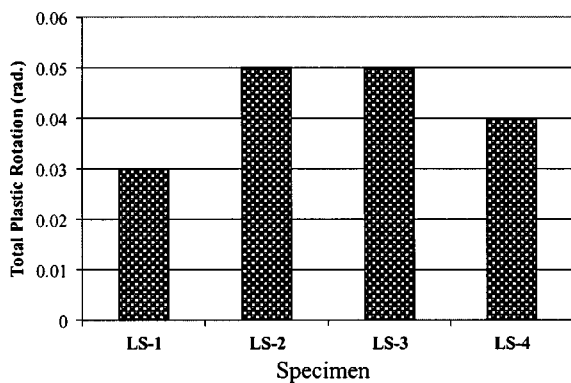


Fig. 7 Comparison of total plastic rotations capacities

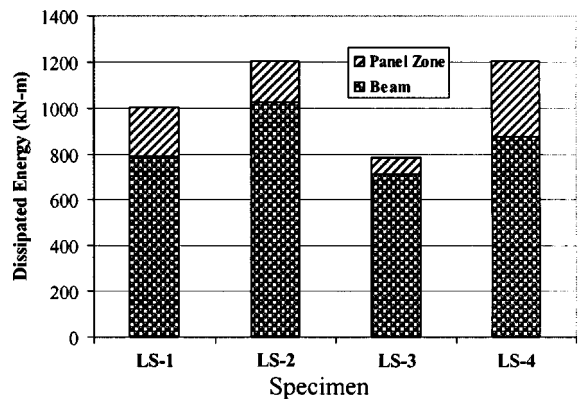


Fig. 8 Comparison of energy dissipation

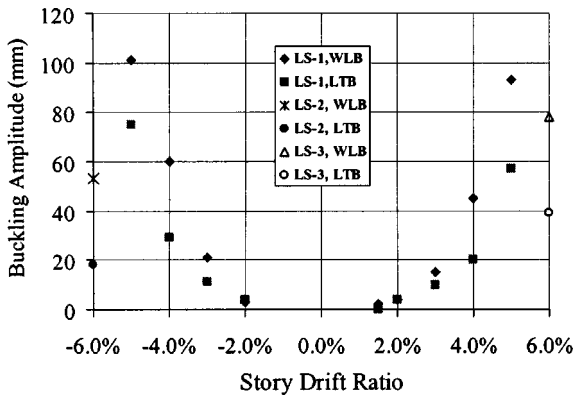


Fig. 9 Comparison of buckling amplitudes

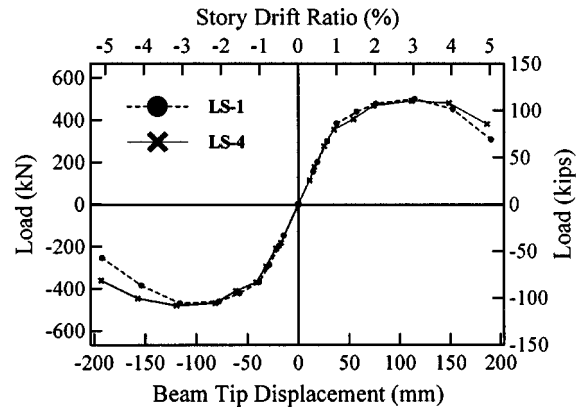


Fig. 10 Response envelopes of specimens LS-1 and LS-4

fault ground motions. Because the standard loading protocol introduces more cumulative damage to the connection before a high displacement is reached, it is prudent not to compare the plastic rotation capacity obtained from the standard loading protocol testing with the demand produced by near-fault ground motions.

Fig. 8 presents the amount of energy dissipated by each specimen. The majority of energy dissipation took place in the beam at the RBS region. The average energy dissipation capacities as obtained from both the standard and near-fault loading protocols were similar.

## 5.2. Buckling amplitudes

The first three specimens did not have lateral bracing near the RBS region. A comparison of the buckling amplitude of these specimens at first cycle of each drift level is included in Fig. 9. Specimen LS-1, tested with the standard loading history, experienced higher buckling amplitudes at 5% drift than those of the near-fault specimens (LS-2 and LS-3) at 6% drift. Because the 6% excursion in the near-fault loading protocol was not preceded by a number of inelastic cycles, the buckling amplitudes of the near-fault specimens were lower.

## 6. Implications of extra lateral bracing effects

Both specimens LS-1 and LS-4 were tested with the standard loading protocol, but LS-4 had an extra bracing near the RBS region. They both completed the 5% drift cycles. Therefore, a direct comparison of the responses can be made for the lateral bracing effect.

### 6.1. Load-displacement envelopes

Fig. 10 shows a comparison of the load-displacement envelopes of both specimens. Note that lateral bracing did not increase the maximum strength of the beam (i.e., the force demand in the beam flange groove welds was not increased). The response envelopes are similar up to 3% drift, beyond which strength degradation took place due to beam buckling (see Fig. 11). The beneficial

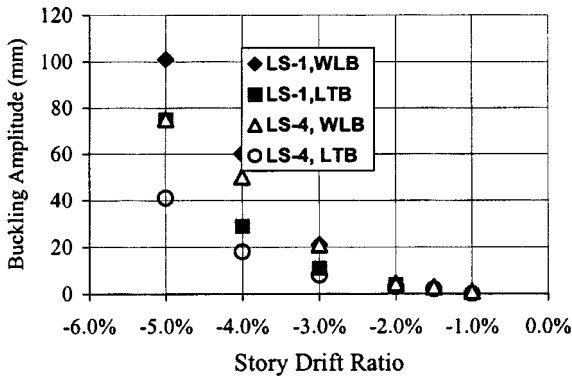


Fig. 11 Comparison of buckling amplitudes

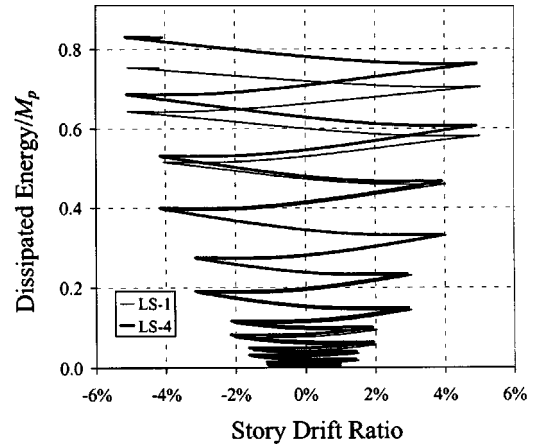


Fig. 12 Comparison of energy dissipation capacities

effect of providing lateral bracing near the RBS region to reduce the rate of strength degradation became significant beyond 3% drift.

### 6.2. Plastic rotation

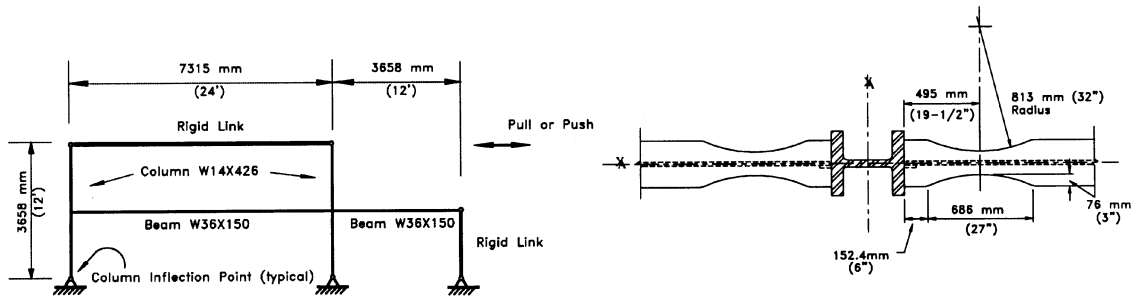
Specimen LS-1 reached 0.03 radian total plastic rotation. The plastic rotation in the panel zone was about 0.01 radian in both specimens. The total plastic rotation of Specimen LS-4 reached 0.04 radian because the capacity of the beam degraded at a slower rate. Had the connection of the lateral bracing not failed, it was likely that the plastic rotation would have reached 0.05 radian.

### 6.3. Energy dissipation

Fig. 8 shows that LS-4 dissipated 20% more energy than LS-1, but the beam component of both LS-1 and LS-4 dissipated about the same amount of energy. But the panel zone of LS-4 dissipated 50% more energy more than that in LS-1. Because the strength degradation was slower in LS-4, the panel zone continued to experience larger deformations at higher drift levels, resulting in larger energy dissipation in the panel zone. Fig. 12 compares the energy dissipation histories up to two cycles of 5% drift. Up to 4% drift, the total energy dissipation was similar for both specimens. The effect of lateral bracing on energy dissipation became significant beyond 4% drift.

### 6.4. Buckling amplitudes

A comparison of the buckling amplitudes of both specimens at each drift level is shown in Fig. 11. Regardless of the presence of extra lateral bracing near the RBS, web local buckling occurred at 1.5% drift in both specimens, which was then followed by lateral-torsional buckling at 2% drift. The WLB amplitudes as well as the LTB amplitudes were very similar at 3% drift. Beyond 3% story drift ratio, however, the extra lateral bracing near the RBS region was effective in reducing the amount of buckling distortions. The buckling of Specimen LS-1 was much more pronounced than that of Specimen LS-1 at 5% drift.



(a) Single-story One-and-a-half-bay Beam-column Assembly      (b) RBS Moment Connection Details

Fig. 13 Structural assembly and connection details

## 7. System restraint effects

### 7.1. Introduction

A typical setup for the one-sided steel moment connection test is shown in Fig. 1, where the beam is cantilevered from the column. At higher deformation levels, strength degradation would occur due to beam buckling. To accommodate the buckling, laboratory observations show that the beam is

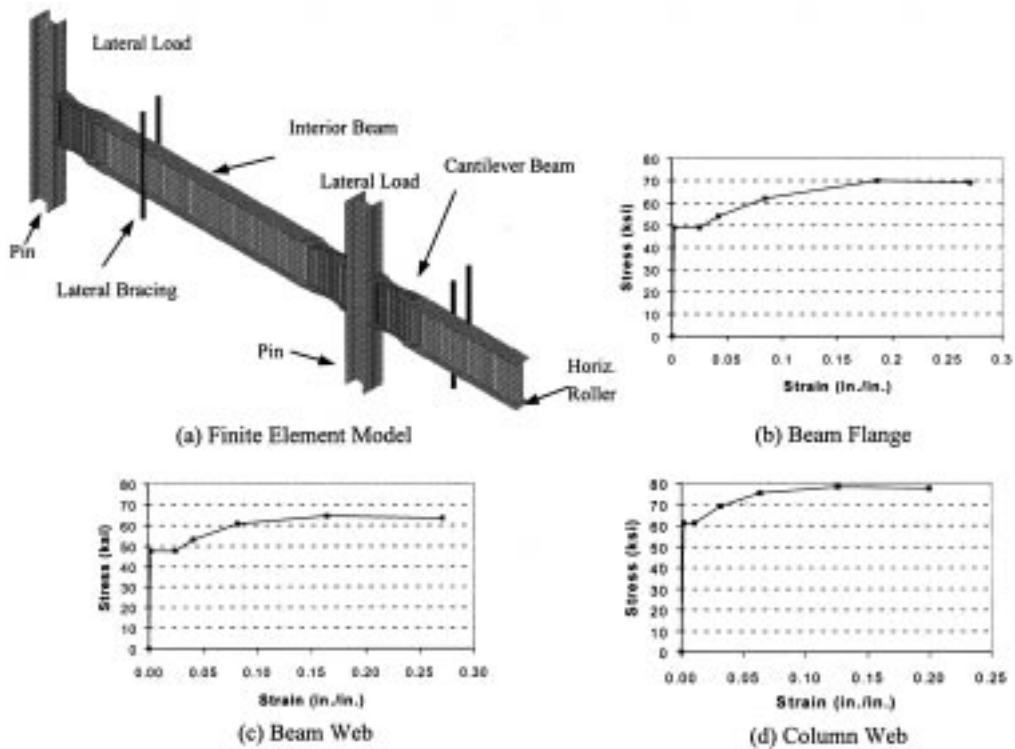


Fig. 14 Finite element model and assumed true stress vs. true strain relationships

shortened. In an actual building frame, however, the beam is restrained axially at both ends by the columns. Therefore, the amount of buckling or strength degradation observed in laboratory testing may be exaggerated. Since it is costly to conduct a system test, an analytical study was performed to evaluate the system restraint effect.

Fig. 13 shows the model that simulates a portion of a multistory frame with RBS moment connections. The frame is composed of one interior beam spanning between two columns. Unlike the interior beam which is restrained axially by the columns, only one-half length of the adjacent interior beam with an assumed inflection point at midspan is included in the model; this half-span beam could shorten freely due to the way that the assembly free-body is extracted from the multistory frame. To simulate the seismic effect, an equal amount of lateral displacement is imposed to the top end of both columns. Thus, comparing the responses of moment connections in both beams can assess the system restraint effect.

## 7.2. Finite element modeling

The ABAQUS finite element analysis program (ABAQUS 1995) was used to model the assembly for large-deformation nonlinear analyses. Fig. 14(a) shows the mesh of the finite element model. A quadrilateral 4-node thin shell elements (element type S4R5 in ABAQUS) with 5 degrees of freedom per node (i.e., three translational components and two in-plane rotations) was used in the modeling of the beams and columns. Each element was divided into five layers through the thickness of the element. The reduced integration scheme with one Gauss integration point in the center of each layer was used to formulate element properties. A more refined mesh was used in the RBS region. The beam flanges and web were fully connected to the column flange, that is, the beam flange weld access holes and the beam web bolted connection were not modeled.

Both columns were supported at the base by a hinge, while the cantilever beam end was supported by a horizontal roller to allow for axial shortening. The beams were braced laterally at locations 2438 mm (8 ft) from the column face. Elastic material properties [i.e., Young's modulus= 200 MPa (29,000 ksi), Poisson's ratio=0.3] were assigned to the portions of the model that were not expected to yield. Nonlinear material properties (see Fig. 14) idealized from tensile coupon test results of a research project (Yu *et al.* 1997) were assigned to the elements in the regions expected to yield. The plasticity model was based on the von Mises yielding criteria and the associated flow rule. Both columns were loaded by simultaneously imposing an equal column tip displacement from zero to 152 mm (6 in).

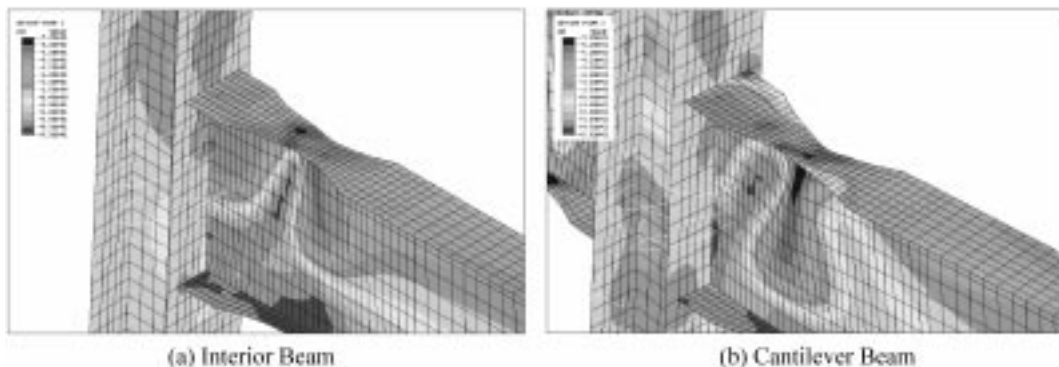


Fig. 15 RBS beam deformation configurations (at 4% Drift)

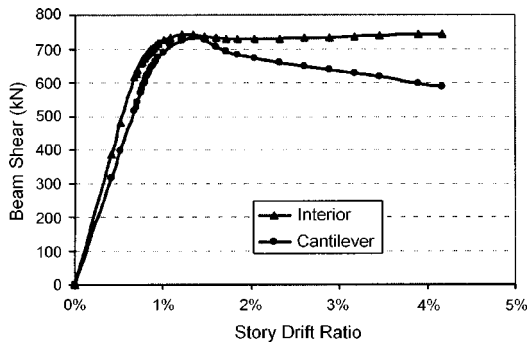


Fig. 16 Beam shear vs. story drift relationships

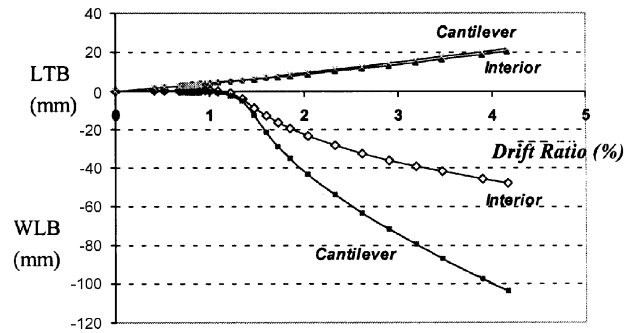


Fig. 17 Comparison of buckling amplitudes

Because strength degradation due to buckling was expected to occur, the standard Newton method, which fails (i.e., diverges numerically) near the limit point of the force-displacement curve, was not adopted to solve numerically the non-linear equilibrium equations. Instead, an algorithm called the modified Riks method was implemented to avoid the divergence near the limit point.

### 7.3. Analysis results

Fig. 15 shows the predicted deformation configurations of both beams at 4% drift. Buckling was less severe in the restrained interior beam. While the cantilever beam showed strength degradation, this was not the case for the interior beam (see Fig. 16). Fig. 17 shows the buckling amplitudes of both beams. At 4% story drift level, the WLB amplitude of the restrained beam was about half that of the cantilever beam. The slab that exists in an actual building may also increase the axial restraining effect. As a parametric study, a separate analysis was performed by constraining equal lateral displacement at both ends of the interior beam. The results were very similar to the case without such constraint.

A recent study conducted by Uang and Fan (1999) indicated that the web local buckling was the controlling factor for the plastic rotation capacity of an RBS connection. With the added benefit from the system restraining effect in an actual building, it appears that extra bracing near the RBS region is unwarranted if the conventional lateral bracing requirement (AISC 1997) is satisfied. However, if it is desirable to control the amount of buckling, adding extra lateral bracing near the RBS can be considered as one option to improve the seismic performance of RBS moment connections. Another situation that may require extra bracing near the RBS is when deep-section columns are used (Gilton *et al.* 2000).

## 8. Conclusions

Cyclic testing of four full-scale RBS moment connections was conducted to evaluate the effect of near-fault ground motions and the effect of adding extra bracing near the RBS region. A non-linear finite element analysis of a one-and-a-half-bay beam-column assembly representing a portion of a multistory frame was also conducted to assess the system axial restraining effect on the behavior of RBS moment connections. The following conclusions can be made.

- 1) All four specimens were able to reach at least 0.03 radian plastic rotation needed for Special Moment-Resisting Frames (SMRFs) without experiencing weld fracture. The connection was capable of delivering a larger plastic rotation capacity (at least 0.05 rad.) when subjected to a near-fault loading history.
- 2) The energy dissipation capacity of the RBS connection was insensitive to the type of loading history used. Adding extra lateral bracing did not affect energy dissipation up until 4% drift, but the energy dissipation was larger at higher drift levels.
- 3) Adding lateral bracing near the RBS region did not increase the beam maximum strength (i.e., the force demand in the welded joints) because strength degradation started to occur before lateral bracing became effective. However, it would further increase the plastic rotation capacity because the strength degradation occurred at a slower rate.
- 4) The system axial restraining effect could significantly reduce the WLB amplitude, and, therefore, the strength degradation at higher displacement levels was significantly reduced. For an SMRF building where axial restraint typically exists, adding lateral bracing near the RBS region appears unwarranted for the connection to deliver 0.03 radian plastic rotation. However, when it is desirable to control the beam distortion in an RBS beam, which is more prone to buckling, adding lateral bracing near the RBS region is beneficial. Another situation where extra bracing may be required is when deep-section columns are used.

## **Acknowledgements**

SAC Joint Venture with Mr. James O. Malloy as the Project Director of Topical Investigations funded this research. The authors would like to thank Nucor-Yamato Steel, AISC, PDM/Stoical, Asbury Steel, and TSI Inc. for their contributions to this project. Mr. Chad Gilton assisted in the testing program.

## **Reference**

- ABAQUS (1995), *Users Manual, I and II*, Version 5.6, Hibbitt, Karlsson & Sorensen, Inc., Providence, RI.
- AISC (1993), *Load and Resistance Factor Design Specification for Structural Steel Buildings*, American Institute of Steel Construction, Chicago, IL.
- AISC (1997), *Seismic Provisions for Structural Steel Buildings*, American Institute of Steel Construction, Chicago, IL.
- AISC (1997), Shape Material (ASTM A572 Gr. 50 with Special Requirements), *Technical Bulletin No. 3*, American Institute of Steel Construction, Chicago, IL.
- Anderson, J.C. and Bertero, V.V. (1987), "Uncertainties in establishing design earthquakes", *Journal of Structural Engineering*, ASCE, **113**(8), 1709-1724.
- Chen, S.-J., Yeh, C.H. and Chu, J.M. (1996), "Ductile steel beam-to-column connections for seismic resistance," *Journal of Structural Engineering*, ASCE, **122**(11), 1292-1299.
- Clark, P., Frank, K., Krawinkler, H. and Shaw, R. (1997), "Protocol for fabrication, inspection, testing, and documentation of beam-column connection tests and other experimental specimens", Report No. SAC/BD-97/02, SAC Joint Venture, Sacramento, CA.
- Engelhardt, M.D. (1999), "Design of reduced beam section moment connections", *Proceedings*, North American Steel Construction Conference, 3-29-1999, AISC, Chicago, IL.
- Engelhardt, M.D., Winneberger, T., Zekany, A.J. and Potyraj, T. (1998), "Experimental investigation of dogbone moment connections", *Engineering Journal*, AISC, **35**(4), 128-139.

- Gilton, C., Chi, B. and Uang, C.-M. (2000), "Cyclic response of RBS moment connections: Weak-axis configuration and deep column effects", Report No. SSRP 2000/03, University of California, San Diego, CA.
- Hall, J.F. (1998), "Seismic response of steel frame buildings to near-source ground motions", *Earthquake Engineering & Structural Dynamics*, **27**(12), 1445-1464.
- Krawinkler, H. and Gupta, A. (1998), "Story drift demands for steel moment frame structures in different seismic regions", *Proceedings, Sixth U.S. National Conference on Earthquake Engineering*, Earthquake Engineering Research Inst., CA, 12 pp.
- Plumier, A. (1997), "The dogbone: back to the future", *Engineering Journal*, AISC, **34**(2), 61-67.
- SAC 1996, "Interim guidelines advisory No. 1", Report No. FEMA-267A, SAC Joint Venture, Sacramento, CA.
- Uang, C.-M. and Fan, C.-C. (1999), "Cyclic instability of steel moment connections with reduced beam sections", Report No. SSRP-99/21, University of California, San Diego, CA.
- Yu, Q.-S., Noel, S. and Uang, C.-M. (1997), "Experimental studies on seismic rehabilitation of pre-Northridge steel moment connections: RBS and Haunch Approach", Report No. SSRP-97/08, University of California, San Diego, CA.
- Yu, Q.-S., Gilton, C.S. and Uang, C.-M. (1999), "Cyclic response of RBS moment connections: loading sequence and lateral bracing effects", Report No. SSRP 99-13, University of California, San Diego, CA.
- Zekioglu, A., Mozaffarian, H., Chang, K.L., Uang, C.-M. and Noel, S. (1997), "Designing after Northridge", *Modern Steel Construction*, AISC, **37**(3), 36-42.